Temporal zeta potential variations of 45S5 bioactive glass immersed in an electrolyte solution

Helen H. Lu,* Solomon R. Pollack, Paul Ducheyne
Center for Bioactive Materials and Tissue Engineering, Department of Bioengineering, University of Pennsylvania, 3320 Smith Walk, Philadelphia, Pennsylvania 19104

Received 6 May 1999; revised 28 October 1999; accepted 16 November 1999

Abstract: 45S5 bioactive glass (BG) is a bioactive material known to bond to bone *in vivo* through a surface calcium phosphate (Ca-P) layer. The goal of this study was to address the importance of BG surface charge in the bioactive response by examining the relationship between charge variations and the formation of the surface Ca-P layer. The zeta potential of BG in an electrolyte solution (TE) was measured by particle electrophoresis, and the formation of a Ca-P layer was characterized using SEM, EDXA, and FTIR. Si, Ca, and P solution concentrations also were determined. The initial BG surface was negatively charged, and two sign reversals were detected during 3 days of immersion. The first, from negative to positive after 1 day, is attributed to the adsorption of cations at the BG surface, and the second reversal was due to the precipitation of phosphate ions from solution. A strong correlation was found between the formation of a Ca-P layer and BG surface zeta potential variations. The dynamic shift in zeta potential from an initially negative surface to a positively charged surface directly corresponded with the formation of an amorphous Ca-P layer. In addition, when the glass surface matured into a crystalline Ca-P layer, it was associated with a reversal from a positive to a negative surface. Future work will focus on the effects of protein adsorption on BG surface charge and Ca-P layer formation kinetics as well as on cellular response to a changing BG surface. © 2000 John Wiley & Sons, Inc. J Biomed Mater Res, 51, 80–87, 2000.

Key words: bioactivity; bioactive glass; surface charge; zeta potential; calcium phosphate layer

INTRODUCTION

45S5 bioactive glass (BG) is a bioactive material capable of establishing a chemical bond to bone *in vivo*.[1] Bioactivity is defined here as the ability of an already biocompatible material to enhance bone formation and to bond to surrounding bone tissue. BG currently is the most bioactive material available.[2] While the events taking place at the interface between BG and bone have been extensively documented, the precise mechanisms associated with its bioactivity have not been fully understood.[2–10] In solution, the surface of BG undergoes a time-dependent modification. A series of solution- and cell-mediated surface reactions result in the formation of a calcium phosphate (Ca-P) layer through which a bond to the surrounding bone tissue is established. The formation of a Ca-P layer *in vitro* on a material surface is believed to indicate its bioactive potential *in vivo*.[2,5] Clearly, a bioactive behavior is an interface-driven phenomenon. Parameters such as surface charge, composition, structure, and morphology will be important in the formation of the Ca-P layer as well as in the interaction between the material surface and the surrounding medium, proteins, and cells.

In this study, experimental results will focus on surface charge for several reasons. BG surface charge, reflected in its zeta potential, expands the characterization of the surface by embodying both solution- and substrate-related reactions. In addition, surface-charge-associated processes are believed to be important in normal biological bone synthesis and remodeling.[12] Previous work from this laboratory demonstrated zeta potential variations of both stoichiometric and calcium-deficient hydroxyapatite (CDHA) as a function of time in 0.01*N* of HNO_3–0.01*N* of KOH. It was found that the time needed to achieve a steady-state zeta potential for the biologically more active CDHA was significantly longer than the time needed to achieve a steady-state zeta potential for stoichiometric HA. It was suggested that these measured dif-

*Present address: Center for Advanced Biomaterials and Tissue Engineering, Department of Chemical Engineering, Drexel University, 3141 Chestnut Street, Philadelphia, Pennsylvania 19104

Correspondence to: H.H. Lu; e-mail: hlu@drexel.edu

Contract grant sponsor: NSF: contract grant number: BCS-92-02314

ferences either influenced or resulted from the ion exchange reactions occurring between the ceramic and the solution.[13] Similarly, in the present study the quantification of BG surface zeta potential variations in an electrolyte solution may shed light on the ion exchange, dissolution, and precipitation reactions that are instrumental in the bioactive response.

The significance of surface charge in the formation of an apatite layer and surface interactions with the cellular environment have been emphasized by many.[3,4,14–18] Li et al. suggested that successful candidate materials for bone bonding either already must have or they must develop negatively charged surfaces with abundant OH^- groups.[15] In another study, hydroxyapatite was induced to form *in vitro* on 100% silica gels.[19] The authors believed that this was possible due to the negatively charged surface and the presence of silanol ($SiOH^-$) groups on the gel surface. The net negative charge of the surface enabled it to attract cations such as Ca^{2+} from solution and, in turn, facilitated apatite deposition.

At this time there have not been any studies reported that quantified the variations in BG surface charge as a function of time in simulated physiologic solutions. The aforementioned studies did not delineate the conditions under which BG will achieve a negative surface potential, nor did they provide any quantitative data on the electronegativity of the bioactive surface in solution. In addition, previous studies have failed to specify the conditions under which the BG surface will exhibit a negative potential. Therefore it is apparent that quantitative explorations of both areas may be crucial in understanding the phenomenon of bioactivity.

We hypothesize that time-dependent variations in BG zeta potential correspond to, and may directly influence, Ca-P layer formation. In this study, we will quantify BG surface zeta potential variations in a physiologic, electrolyte solution and, subsequently, we will relate these variations to the concurrent formation of the Ca-P layer on the BG surface.

MATERIALS AND METHODS

Sample preparation

45S5 bioactive glass particles (wt %: 45.2% SiO_2, 24.2% Na_2O, 24.6% CaO, and 6.0% P_2O_5), about 10 μm in size, were used in this study (Orthovita, Malvern, Pennsylvania). The as-received glass was analyzed by X-ray diffraction (Rigaku-Geigerflex diffractometer) and found to be amorphous in structure. A qualitative examination of the particles by scanning electron microscopy confirmed the largest dimension of the majority of the particles to be less than 10 μm.

The electrolyte solution used for the immersion experiment was based on 0.05*M* of tris hydroxymethyl aminomethane/HCl buffer (tris buffer; Sigma Chemicals, St. Louis, Missouri), with a solution ion concentration and composition similar to that of human blood plasma. Specifically, the solution used here, tris buffer plus electrolytes (TE), maintained a pH of 7.4 at 37°C, was composed of 152.0 m*M* Na^+, 135.0 m*M* of Cl^-, 5.0 m*M* of K^+, 2.5 m*M* of Ca^{2+}, 27.0 m*M* of HCO_3^-, 1.5 m*M* of Mg^{2+}, 0.4 m*M* of SO_4^{2-}, and 1.0 m*M* of $H_2PO_4^{-1}$. In addition, the solution had an ionic strength of 0.17*M*.

BG particles were immersed in TE at a weight-to-solution-volume ratio of 1.0 mg/mL. Each sample was incubated at 37°C for 0.25, 0.5, 1, 2, 3, 4, 5, or 12 h, or 1, 3, or 7 days. Unreacted BG and TE without BG served as controls.

Zeta potential measurement

When a BG particle is suspended in a polar medium, a surface electric double layer develops that governs the ion distribution from the particle surface into the solution.[20] The electric potential at the hydrodynamic boundary separating the two layers is defined as the zeta potential of the surface. The magnitude and sign of the zeta potential provide valuable information regarding the electric charge present at the interface between the glass and the solution.

In this study, the zeta potential of bioactive glass (BG) particles was measured using the Pen Kem System 3000 electrokinetic analyzer (Pen Kem Inc., Bedford Hills, New York). The theory of particle electrophoresis and operation of the analyzer have been described elsewhere.[13,22,23] Briefly, BG particles loaded into the quartz capillary chamber were set into motion by an applied electric field. The instrument determined the velocity of the particle motion by reflecting a laser beam from the moving particles and passing the light through a rotating radial grating and into a photomultiplier tube. The photomultiplier tube voltage is proportional to the incident light intensity, which. in turn, is a function of particle surface area and the reflective index of the particles. This information, after fast Fourier analysis, was converted into an electrophoretic mobility histogram of the particles, and the peak value in the histogram was used to calculate the zeta potential via the Smulochowski equation.[21]

In general, most particles can be treated as either elliptical cylinders or spheroids. The Smulochowski equation, employed in this study to relate particle electrophoretic mobility to zeta potential, holds for a nonconducting particle of any shape provided that the radius of curvature at all points on the particle is large compared to the thickness of the electric double layer. This applies to the 45S5 bioactive glass particles studied here since the effective size of the particle is much greater than the thickness of the surrounding double layer. Moreover, Overbeek et al.[36] have shown that distortion of the electric field, or of the double layer surrounding the particle when it travels through the fluid, is negligible for any particle shape if the thickness of the double layer is much smaller than any radius of the curvature of the particle.

In addition, the experiments and acquisition of the zeta potential were designed to minimize variations originating from differences among particles. For each time point examined, the zeta potential data (n = 9) presented here were

calculated from average electrophoretic mobility values based on nine separate histograms. Moreover, the average electrophoretic mobility was calculated based on the mobility of all the particles ($n > 50$) present in the electrophoresis chamber during each measurement.

Surface analyses (FTIR, SEM, EDXA)

At the end of each immersion period, the particles were separated from solution by centrifugation (Adams analytical centrifuge, 3400 rpm). The samples immediately were washed with methanol to prevent further reaction and left to dry overnight in a 37°C oven. Subsequently the surfaces were analyzed by Fourier transform infrared spectroscopy (FTIR; Nicolet 5DXC spectrometer, Madison, Wisconsin) in the diffuse reflectance mode. The glass particles were embedded in KBr, and spectra were obtained with 300 scans per sample at a resolution of 4 cm^{-1}.

Surface morphology and composition before and after immersion in TE were studied using scanning electron microscopy (SEM; JEOL JSM 6300, 2 kV) and energy dispersive X-ray analysis (EDXA; JEOL JSM 6400, 10 kV). The samples were coated with carbon to eliminate any charging effects.

Solution analyses (pH, Ca, PO_4, and Si concentrations)

Solution pH was measured at 37°C (Brinkmann 632 digital pH meter) prior to centrifugation. After separation of the particles from solution, calcium and silicon concentrations in the postimmersion solution were measured by flame atomic absorption spectroscopy (Perkin–Elmer Model 5100, Norwich, Connecticut). Prior to measurement, the system was calibrated using Ca or Si standard solutions.

Phosphorous concentration was determined in a colorimetric assay[24] by measuring the concentration of the phospho–molybdate complex using a UV-visible spectrophotometer (Biochrom, LKB 4053 Ultrospec K). Three separate trials were conducted, and three individual samples were analyzed per time point. Concentrations at each time point were measured in triplicate and the mean and standard deviation calculated.

RESULTS

Zeta potential measurements

Time-dependent changes in BG zeta potential in TE are shown in Figure 1. Each data point represents the mean of nine zeta potential values calculated based on the average EPM of nine histograms ($n = 9$). The error bar represents the standard deviation of the mean. The data are indicative of a dynamic surface, as two sign reversals in BG surface zeta potential were measured after 3 days in TE. The initial BG surface was negative in charge, with an average zeta potential of −14.7 mV. However, as time progressed, the surface became increasingly positive, and after 1 day, it measured an average zeta potential of +7.5 mV. The surface was negatively charged after 3 days of immersion, and it remained negative after 7 days in TE.

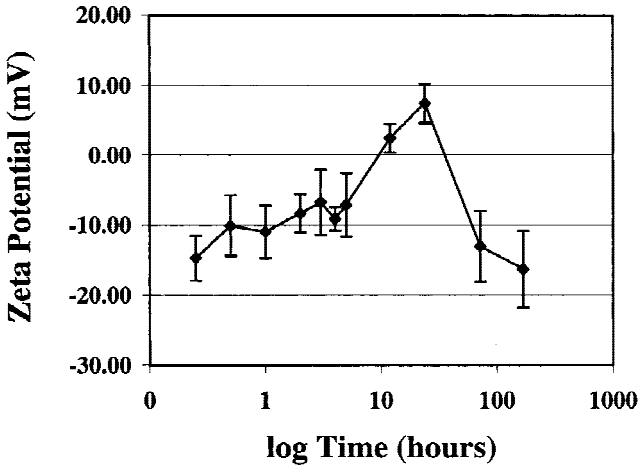

Figure 1. 45S5 bioactive glass (BG) zeta potential as a function of immersion time in an electrolyte solution (TE). The immersion ratio equals 1 mg/mL. Each data point in the graph is calculated based on the average electrophoretic mobility values obtained from nine sets of electrophoretic mobility histograms (n = 9). The error bars represent standard deviations of the means.

FTIR analysis

FTIR was used to monitor the formation and growth of the Ca-P layer on BG by detecting characteristic vibration modes of the P-O and P=O bonds. Of interest here was the appearance of a P-O bending vibrational band between 600 and 570 cm^{-1}, indicative of the presence of amorphous calcium phosphate on the surface. In addition, a particle-size associated peak occurred between 810 and 800 cm^{-1}. Figure 2 compares FTIR spectra of BG immersed in TE as a function of immersion time (0 h, 1 day, 3 days, and 7 days). An amorphous Ca-P layer was seen after 1 day of immersion, and 2 days later it developed into a crystalline Ca-P layer, as indicated by the divided P-O bending vibration peak between 600 and 500 cm^{-1}. A C-O stretching vibration appeared between 890 and 800 cm^{-1} after 3 days, suggesting the presence of carbonated Ca-P on the BG.[2,10,25,26]

SEM/EDXA analyses

The most notable feature in SEM images of reacted BG samples was the accumulation of surface nodules after only 15 min in TE. As immersion continued, the

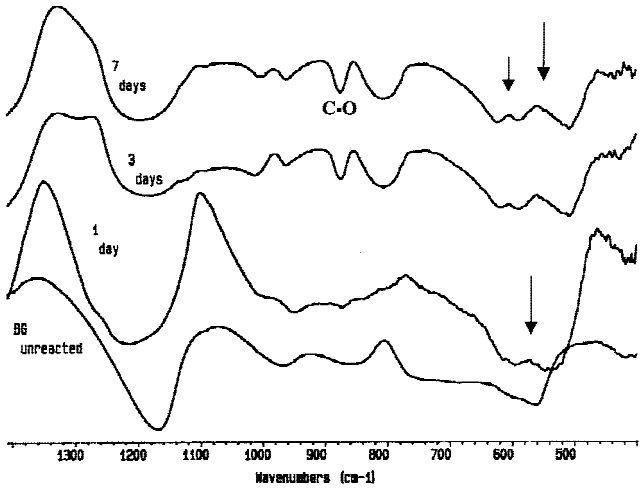

Figure 2. Fourier transform infrared (FTIR) spectra of unreacted 45S5 bioactive glass (BG) and of BG after immersion in an electrolyte solution (TE) for 1 day, 3 days, and 7 days. Note the appearance of the P-O bending vibrational band between 600 and 500 cm^{-1} after 1 day, suggesting that an amorphous calcium phosphate (Ca-P) layer had been formed on the surface. This peak became divided after 3 days, indicative of the formation of a crystalline Ca-P layer.

sample surface became increasingly covered with these nodules, and they later merged to form larger particles that populated the glass surface, as seen in Figure 3. EDXA analysis showed the nodules to be made up largely of Ca; smaller amounts of Si and P were present at very low levels initially.

EDXA revealed that the reacted glass surface was comprised of Na, Si, Ca, P, and Cl, with each element present at varied peak intensities as a function of time. The unreacted BG surface was made up of Na, Si, Ca, and P. After the BG was exposed to TE, the intensity of the Na peak diminished and became undetectable after 3 h of immersion, while Cl, absent in the spectrum for unreacted glass, was detectable after 12 h in TE. Figure 4 shows two typical EDXA spectra of BG immersed in TE for (a) 1 day and (b) 3 days. Although the peak intensity of each element could not be quantified in the absence of a comparable standard, the relative intensity ratios of the elements in an EDXA spectrum may be compared to the same elemental ratios found in another spectrum. As immersion continued, we found that the Ca/P ratio decreased from 4.0 for unreacted BG to 1.7 for the 1-day reacted surface and, later, to 1.5 for the 3-day sample. The time-dependent decrease in surface Ca/P ratio implies an increasing presence of phosphorus on the surface.

Solution analyses

Si dissolution was observed at the start of immersion, and its concentration increased from 0.07 m*M* in

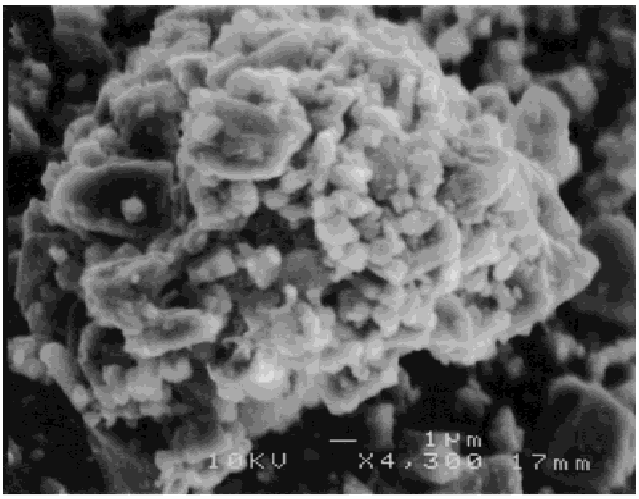

(a)

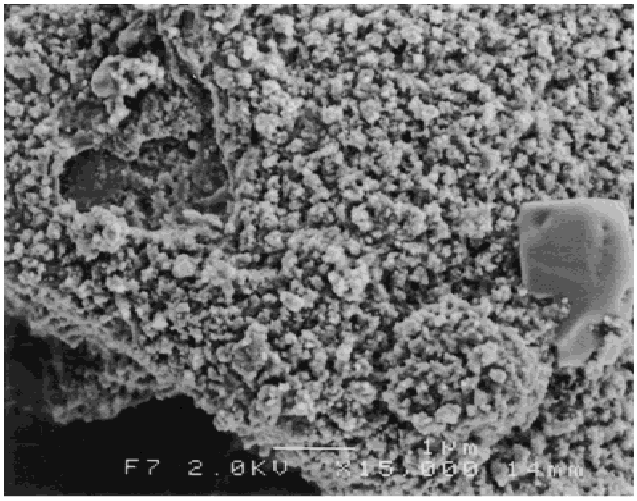

(b)

Figure 3. Scanning electron microscopy (SEM) images of 45S5 bioactive glass (BG) immersed in an electrolyte solution (TE) for (a) 1 day and (b) 3 days. At 1 day, note the appearance of sub-micron nodules on the BG surface. The nodules was made up of Si, Ca, and P (original magnification ×4,300). After 3 days, the surface was covered with Ca-P nodules, which had aggregated to form larger structures (original magnification ×15,000).

TE to 2.1 m*M* after 1 day. Subsequently no additional Si was released as the Si solution concentration stabilized between 2.1 and 2.2 m*M* after 1 day in TE. The Ca solution concentration increased from 2.5 m*M* in the control TE solution to 3.6 m*M* after the BG was in TE for 15 min. The leaching continued, and after 24 h the Ca concentration reached 4.2 m*M*. However, from that point on, the calcium concentration decreased to about 3.0 m*M* on day 7, suggesting the precipitation of calcium ions onto the glass surface.

There was no large initial release of phosphorous ions by the glass particles; the P concentration increased only about 0.15 m*M* after 15 min, as shown in Figure 5. This trend continued for the next 4 h. How-

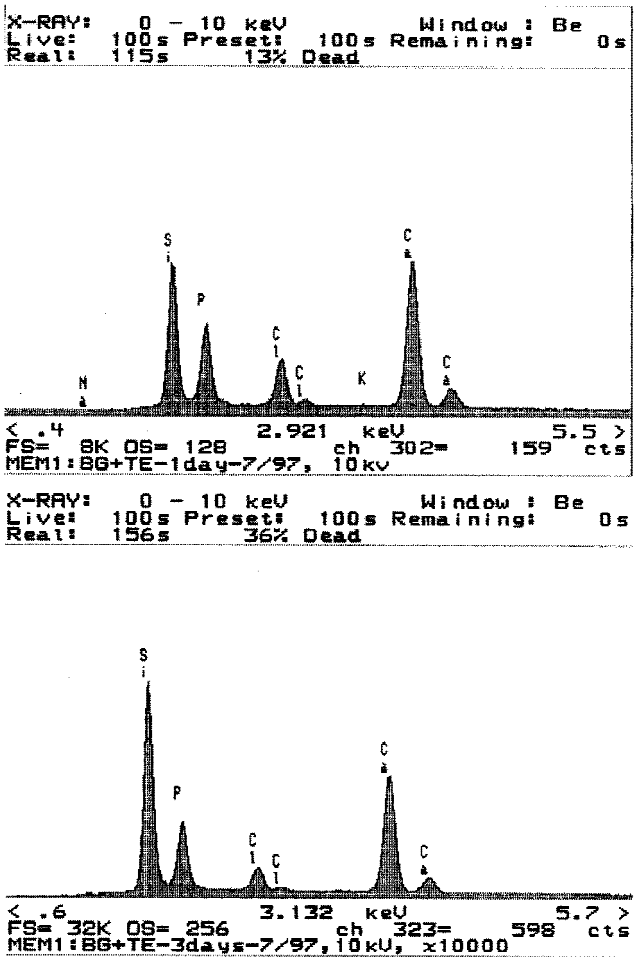

Figure 4. Energy dispersive X-ray analysis (EDXA) spectra of 45S5 bioactive glass (BG) immersed in an electrolyte solution (TE) for (a) 1 day and (b) 3 days. After 1 day, Si, Ca, P, and Cl were found on the surface, but the Na peak had disappeared. After 3 days, Si continued to be present at high intensities on the BG surface, and the peak intensity of P had increased relative to the other elements.

ever, after 5 h in TE, an uptake of phosphorous from the solution was measured. After 12 h, about 0.26 m*M* had been depleted from the solution, and 7 days later the solution was almost completely free of phosphorus ions.

DISCUSSION

One of the objectives of this study was to examine the relationship between measured BG surface charge variations and the concurrent formation of a surface Ca-P layer. Our data suggest a strong correlation between glass surface Ca-P layer formation and zeta potential changes as measured in an electrolyte solution. The observed variations in BG zeta potential over an immersion period of 7 days in TE evidence gradual changes within the electric double layer at the interface between BG and the solution. The dynamic shift in BG zeta potential from an initially negative surface to a positively charged surface directly corresponded with the formation of an amorphous Ca-P layer detected after 24 h of immersion. In addition, when the glass surface matured into a crystalline Ca-P layer after 3 days of immersion, we measured a reversal from a positive to a negative surface zeta potential within the same time frame.

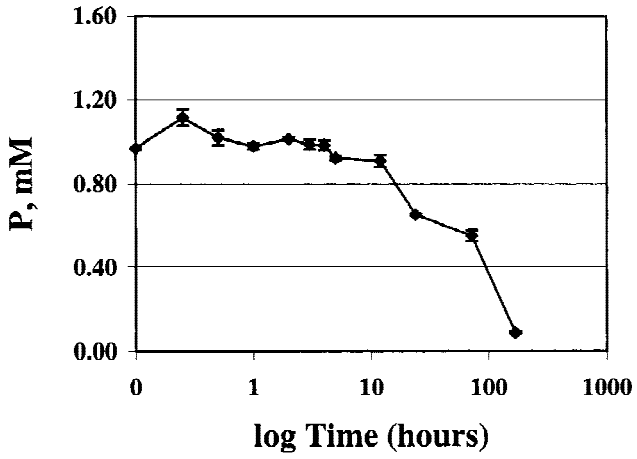

Figure 5. Phosphorous (P) solution concentration as a function of time after the 45S5 bioactive glass particles (BG) had been immersed in an electrolyte solution (TE). Immersion ratio = 1 mg/mL, n = 3. The error bars represent standard deviations of the means.

In vitro, a series of diffusion, dissolution, and precipitation reactions result in the formation of a Ca-P layer at the glass surface.[3,4] At physiologic pH, the inherently unstable glass structure actively leach Na^+ Si^{4+} and Ca^{2+} ions into solution. Disruption of the glass network, coupled with subsequent condensation and repolymerization reactions, lead to the formation of a silica-rich gel layer on the surface.[2,5,27] On this gel layer, precipitation of calcium and phosphate ions from solution, combined with the migration of these ions from bulk to surface, results in the rapid formation of an amorphous Ca-P layer.[2,5,8,28]

The zeta potential, surface, and solution results of this study, when viewed collectively, confirm the occurrence of the diffusion, dissolution, and precipitation reactions that lead to the formation of a Ca-P layer on BG. FTIR analysis revealed that the Si-O alkali stretch vibrational band located at 930 cm^{-1}, found in unreacted BG, diminished as immersion in TE continued. This change, taken together with the sharpening of the Si-O stretch and Si-O bend bands at 1090 and 470 cm^{-1}, respectively, indicate the occurrence of Si hydrolysis reactions and the leaching of Na^+ and Ca^{2+} ion from the glass into solution. Based on FTIR alone, we cannot directly comment on the formation of the silica-rich gel layer, often suggested by the appearance of a Si-O-Si vibrational band around 800 cm^{-1}. Here the

Si-O-Si band peak coincides with a particle-size associated interference peak found around the same energy region. However, it is well known that the silica gel surface is negatively charged, and we measured a negative BG surface during the initial hours of immersion, within the time frame that the silica gel was believed to be forming.[2] The presence of a negative silica gel layer is likely to promote apatite formation, serving as a surface onto which calcium and phosphate ions could accumulate. SEM images of BG in TE documented the immediate accumulation of calcium phosphate nodules on the glass surface. EDXA data revealed that the reacted glass surface was made up largely of silicon, calcium, and phosphorous, as well as chlorine acquired from solution. The calcium phosphate nodules later aggregated to form larger deposits, and after 1 day of immersion in TE, an amorphous Ca-P layer was detectable on the glass surface by FTIR.

Previously we reported on the kinetic variation of BG zeta potential in de-ionized water.[29] We observed a similar transition from an initially negative to a positive BG surface as immersion proceeded; however, the surface reached positive values in 3 h as opposed to 24 h in TE. BG immersed in tris buffer without electrolytes[29] measured an initially negative surface that later became positive, albeit at a relatively faster pace compared to BG in tris buffer supplemented with electrolytes (TE). In summary, as solution ion concentration increased, the time required to reach a more positive surface lengthened.

The kinetics of Ca-P layer formation on BG is influenced by variations in solution pH, electrolyte concentration, and glass surface area-to-solution volume ratio, as well as the adsorption of serum proteins.[10,30] Kim et al. found that an amorphous Ca-P layer was present on BG after only 1 h of immersion in tris buffer, and a crystalline layer was detected by FTIR 1 h later.[31] Radin et al. showed that a crystalline Ca-P layer was detectable on BG disks only after 3 days of immersion in TE.[10] It is clear that increases in solution complexity delayed the formation of the Ca-P layer, and this delay is reflected in the longer transition time needed for a negative BG surface to revert to a positively charged surface. It also is interesting that the amorphous Ca-P layer detected after 1 day in TE measured a very different zeta potential compared to the crystalline Ca-P layer found at day 3 of immersion. These results suggest that structural variations at the surface may correspond to distinctly different zeta potentials. Ducheyne et al.[13] measured the zeta potential of both stoichiometric and calcium-deficient hydroxyapatite (HA and CDHA) as a function of time in HNO_3-KOH solutions. They found that the zeta potentials of CDHA and HA were different in magnitude, with CDHA measuring a more negative zeta potential than HA under identical immersion conditions.

We hypothesized here that kinetic zeta potential variations corresponded to, and might directly influence, a Ca-P layer formation. The measured shifts in zeta potential reported here undoubtedly reflect the dissolution, precipitation, and ion exchange reaction dynamics at the interface. In addition, the value and sign of zeta potential could determine the charge quantity, distribution, and the types of ion available at the glass–solution interface and consequently alter the kinetics of glass surface transformation into a Ca-P layer. At the interface *in vitro,* the overall solid solution response is, in effect, characterized by four separate reactions: (1) preferential diffusion of alkaline ions; (2) dissolution of silicon; (3) SiO_2 condensation reactions in the formation of the silica gel layer; and (4) precipitation reactions leading to the formation of a Ca-P layer. Of the four reactions occurring at the interface, the zeta potential of BG through electrostatic interactions is likely to play a role in the diffusion, dissolution, and precipitation reactions. The BG surface reactions will result in the rearrangement of ions within the double layer and consequently change the reaction dynamics at the glass–solution interface. In addition, charge-associated electric fields within the electric double layer could affect the rate constants and energetics of interfacial reactions, increasing or lowering the energy barrier for each reaction and, consequently, influencing the formation of a surface Ca-P layer.

Li et al. suggested that signs of the electric potentials at the glass surface would cause ion distribution within the electric double layer to vary from the bulk solution.[18] This difference would, in turn, become instrumental in the formation of a protective layer on the glass. Tanahashi et al.[37] studied apatite formation on self-assembled monolayers (SAMs) of alkanethiols with different surface functional groups and reported that the negatively charged surface groups (PO_4H_2 and COOH) were potent apatite inducers while SAMs with nonionic ($CONH_2$,OH) and positively charged (NH_2) functional groups did not support rapid apatite formation. It is believed that the apatite induction process likely begins with the accumulation of Ca^{2+} on the material surface, with subsequent complexation of phosphate ions. Therefore, a strongly negative surface would promote the formation of surface apatite.

In this study we observed two sign reversals in BG zeta potential within 3 days of immersion in TE. On a mechanistic level, the negative glass surface could trap ions such as Na^+, Ca^{2+}, and Si^{4+} leaching from the bulk glass within the slip plane, and it would attract to the surface cations such as Ca^{2+} from the solution. These actions would result in an increased presence of positive ions at the interface, reflected in the measured reversal from a negative to a positive zeta potential as immersion continued from 15 min to 24 h.

We did not measure the concentration of Na^+ ions in

solution in the present study. However, Andersson et al.[32] examined the solution kinetics of S53P4 (wt %: 53.0% SiO_2, 23.0% Na_2O, 20.0% CaO, and 4.0% P_2O_5) bioactive glass granules immersed in tris buffer. They found that during the first 2 h of immersion, Na^+ ions leached from the bulk glass at a slower rate than Ca^{2+}. The authors suggested that this discrepancy might be attributed to the formation of an electric double layer at the glass–solution interface where the positively charged sodium ions compensated for the negatively charged silica surface. Berretta et al.[23] reported a zeta potential reversal from negative to positive for bovine metatarsal particles exposed to increasing concentrations of NaCl solutions. It was suggested that the super-equivalent adsorption of Na^+ ions might be responsible for the observed shift in polarity of the bone particles. In our study the adsorption of Na^+ ions within the electric double layer contributed to the increasingly positive zeta potential after 1 day in TE. Concurrently, the accumulation of Ca^{2+} ions on the surface also may contribute to the drive towards a more positive zeta potential. Kowalchuk et al.[22] reported that CDHA particles immersed in simulated bone extracellular fluid measured a zeta potential of −11 mV, and it decreased in magnitude and inverted its sign with increasing Ca^{2+} solution concentration. The observed reversal in charge was attributed to the increasing presence of Ca at the interface between the ceramic and the solution.

In the long-term immersions, we measured a second reversal in BG zeta potential value, where it changed from positive on day 1 to negative on day 3. This reversal was caused by the accumulation of phosphate ions to the positively charged 1-day surface. Within the same period, we measured an increase in the phosphorous precipitation, and after 7 days, the solution was nearly depleted of phosphorous. In addition, we found a decrease in Ca/P peak intensity ratio when comparing the day-1 to the day-3 EDXA spectrum. These findings support phosphorus ion accumulation on the BG surface. The adsorption of potential determining, negatively charged, phosphate ions on the BG would lead to the observed electrokinetic sign reversal from a positive day-1 surface to a negative day-3 surface. Similar effects of phosphate ions on both synthetic calcium phosphate surfaces and bone particles have been observed in electrophoretic mobility studies conducted by other researchers.[23,33–35]

The major changes in BG zeta potential as a function of exposure to TE are important observations. The magnitude and sign of the measured BG zeta potential are directly associated with significant electric fields that may have profound effects on cellular function. Biologically, stress-generated potentials in fluid-filled bone are known to derive from electrokinetic effects, where the zeta potential at the bone–fluid interface is the material's property that most strongly influences the amplitude and polarity of the induced electric fields.[12] It is possible that *in vivo* the bioactive surface, exhibiting a negative zeta potential, can act as the surface upon which electrokinetic stimulation of bone growth is possible. Finally, in time the dynamic shifts in BG zeta potential observed here may be translated into significant effects on protein adsorption and cellular activity. Whether BG zeta potential is directly involved in Ca-P layer formation by dominating the forces that drive the accumulation of cations and anions on the glass surface, or whether it is, instead, the result of such accumulations is not yet known.

CONCLUSIONS

By examining the relationship between time-dependent variations in surface charge and the corresponding surface composition, structure, and morphology changes, this study contributes to the elucidation of the underlying mechanisms of bioactivity. We have examined the changing BG surface in an electrolyte solution with an ion concentration similar to that of blood plasma, and we have determined the surface to be negatively charged, as speculated by many authors. We also have demonstrated that BG zeta potential variations directly correspond to surface Ca-P layer formation.

BG zeta potential varied continuously as a function of immersion time and surface and solution composition. We measured two sign reversals in the zeta potential of BG within 3 days of immersion in TE. The first reversal from negative to positive after 1 day of immersion may be attributed to the adsorption of cations within the slip plane. These actions lead to the formation of an amorphous Ca-P layer. The second reversal was due to the precipitation of phosphate ions from the solution, which contributed to the growth and crystallization of the Ca-P layer.

Zeta potential studies, coupled with surface and solution analyses, provide special insight into the dynamic reactions occurring at the BG surface as it develops into a Ca-P layer. Future work will focus on the effects of protein adsorption on BG surface charge and Ca-P layer formation kinetics as well as on cellular response to the changing BG surface.

References

1. Hench LL, Splinter RJ, Allen WC, Greenlee TK. Bonding mechanisms at the interface of ceramic prosthetic materials. J Biomed Mater Res 1971;2(1):117–141.
2. Hench LL. Bioceramics: From concept to clinic. J Am Ceram Soc 1991;74(7):1487–1510.
3. Ducheyne P, Cuckler JM. Bioactive ceramic prosthetic coatings. Review. Clin Orthop Rel Res 1992;102–114.

4. Ducheyne P, Bianco P, Radin S, Schepers E. Bioactive materials: Mechanisms and bioengineering considerations. In: Bone bonding. Reed Healthcare Communications; 1992. p 1–12.
5. Ducheyne P. Bioceramics: Material characteristics versus in vivo behavior. J Biomed Mater Res 1987;21:219–236.
6. Kokubo T, Kushitani H, Ohtsuki C, Sakka S. Chemical reaction of bioactive glass and glass–ceramics with a simulated body fluid. J Mater Sci: Mater Med 1992;3:79–83.
7. Hench LL, Wilson J. Surface-active biomaterials. Science 1984; 226:630–636.
8. Andersson OH, Kangasniemi I. Calcium phosphate formation at the surface of bioactive glass in vitro. J Biomed Mater Res 1991;25:1019–1030.
9. Gross U, Strunz V. The interface of various glasses and glass ceramics with a bony implantation bed. J Biomed Mater Res 1985;19:251–271.
10. Radin S, Ducheyne P, Rothman P, Conti A. The effect of *in vitro* modeling conditions on the surface reactions of bioactive glass. J Biomed Mater Res 1997;37:363–375.
11. Ogino M, Ohuchi F, Hench LL. Compositional dependence of the formation of calcium phosphate films on bioglass. J Biomed Mater Res 1980;14:55–64.
12. Pollack SR. Bioelectrical properties of bone. Endogenous electrical signals. Orthop Clin N Am 1984;15:3–14.
13. Ducheyne P, Kim CS, Pollack SR. The effect of phase differences on the time-dependent variation of the zeta potential of hydroxyapatite. J Biomed Mater Res 1992;26:147–168.
14. van Wagenen RA, Andrade JD. Flat plate streaming potential investigations: Hydrodynamics and electrokinetic equivalency. J Colloid Interface Sci 1980;76(2):305–314.
15. Li P, Ohtsuki C, Kokubo T, Nakanishi K, Soga N, de Groot K. The role of hydrated silica, titania, and alumina in inducing apatite on implants. J Biomed Mater Res 1994;28:7–15.
16. Hench LL, Ethridge EC. Biomaterials: An interfacial approach. New York: Academic Press, Inc.; 1982.
17. Kokubo T. Bioactivity of glasses and glass ceramics. In: Bone bonding. Reed Healthcare Communications; 1992. p 31–46,.
18. Li PJ, Zhang F. The electrochemistry of a glass surface and its application to bioactive glass in solution. J Noncryst Solids 1990;119:112–118.
19. Li P, Ohtsuki C, Kokubo T, Nakanishi K, Soga N, Nakamura T, Yamamuro T. Effects of ions in aqueous media on hydroxyapatite induction by silica gel and its relevance to bioactivity of bioactive glasses and glass–ceramics. J Appl Biomater 1993;4: 221–229.
20. Hunter RJ. Zeta potential in colloid science: Principles and applications. London: Academic Press, Inc.; 1988.
21. Smoluchowski MV. Electrische endosmose und stromungsstrome. In: Handbuch der Electrizitat und des Magnetismus. Leipzig: Barth; 1921. p 366–428.
22. Kowalchuk RM, Pollack SR, Ducheyne P, King LA. Particle microelectrophoresis of calcium-deficient hydroxyapatite: Solution composition and kinetic effects. J Biomed Mater Res 1993;27:783–790.
23. Berretta DA, Pollack SR. Ion concentration effects on the zeta potential of bone. J Orthop Res 1986;4:337–345.
24. Heinonen JK, Lahti RJ. A new and convenient colorimetric determination of inorganic orthophosphate and its application to the assay of inorganic pyrophosphatase. Anal Biochem 1981; 113:313–317.
25. Fujiu T, Ogino M. Difference of bone-bonding behavior among surface active glasses and sintered apatite. J Biomed Mater Res 1984;18:845–859.
26. Ducheyne P, Radin S, King L. The effect of calcium phosphate ceramic composition and structure on *in vitro* behavior. I. Dissolution. J Biomed Mater Res 1993;27:25–34.
27. Pantano CG Jr. Clark AE Jr, Hench LL. Multilayer corrosion films on bioglass surfaces. J Am Ceram Soc—Disc Notes 1974; 57:412–413.
28. Andersson OH, Karlsson KH, Kangasniemi I. Calcium phosphate formation at the surface of bioactive glass in vivo. J Noncryst Solids 1990;119:290–296.
29. Lu H, Pollack SR, Ducheyne P. Particle electrophoresis of 45S5 bioactive glass particles in simulated physiological electrolyte solutions. Proc Surf Biomater 1995:24.
30. Douglas RW, El-Shamy TMM. Reactions of glasses with aqueous solutions. J Am Ceram Soc 1967;50(1):1–7.
31. Kim CY, Clark AE, Hench LL. Early stages of calcium-phosphate layer formation in bioglasses. J Noncryst Solids 1989;113:195–202.
32. Andersson OH, Yrjas KP, Karlsson KH. Reactions in and at the surface of bioactive glasses in aqueous solutions. Bioceramics 1991; 127–133.
33. Leach SA. Electrophoresis of synthetic hydroxyapatite. Arch Oral Biol 1960;3:48–56.
34. Chander S, Fuerstenau DW. On the dissolution and interfacial properties of hydroxyapatite. Coll Surfaces 1998;4:101–120.
35. Guzelsu N, Walsh WR. Streaming potential of intact wet bone. J Biomech 1990;23:673–685.
36. Overbeek, Philips Res. Reports 1946;1:315,
37. Tanahashi M, Matsuda T. Surface functional group dependence on apatite formation on self-assembled monolayers in a simulated body fluid. J Biomed Mater Res 1997;34:305–315.